Received: 27 January 2023 | Accepted: 6 November 2023

DOI: 10.1113/EP091146

Experimental Physiology WILEY

RESEARCH ARTICLE

The algorithm used for the calculation of gas exchange affects the estimation of O_2 uptake kinetics at the onset of moderate-intensity exercise

Maria Pia Francescato | Valentina Cettolo

Department of Medicine, University of Udine, Udine, Italy

Correspondence
Maria Pia Francescato, Department of Medicine, University of Udine, P.le Kolbe 4, 33100 - Udine, Italy.
Email: mariapia.francescato@uniud.it

Funding information
University of Udine, Grant/Award Number: #07/2020_IRB

Handling Editor: David Poole

Abstract

At the start of a moderate-intensity square-wave exercise, after a short delay, breath-by-breath O_2 uptake at the mouth is approximated to a mono-exponential function, whose time constant is considered matched to that of the O_2 uptake of the working muscles. We compared the kinetic parameters obtained from the breath-by-breath gas exchange data yielded by the 'Independent-breath' algorithm (IND), which accounts for the changes in lung gas stores, with those obtained with the classical 'Expiration-only' algorithm (EXP). The two algorithms were applied on the same flow and gas fraction traces acquired on 10 healthy volunteers, performing 10 times the same moderate-intensity exercise transition. Repeated O_2 uptake responses were stacked together and the kinetic parameters of a mono-exponential function were estimated by non-linear regression, removing the data pertaining to 1-s progressively longer initial periods (ΔT_r). Independently of ΔT_r, the mean response time (time constant + time delay) obtained for the IND data was faster compared to the EXP data (~43 s vs. ~47 s, $P < 0.001$), essentially because of shorter time delays. Between $\Delta T_r = 16$ s and $\Delta T_r = 29$s, the time constants of the IND data decreased (30.7 s vs. 28.0 s, $P < 0.05$; drop = 10%), but less than those of the EXP data (32.2 s vs. 26.2 s, $P < 0.001$; drop = 23%); with the same ΔT_r, the time constants of the two algorithms' data were not different ($P > 0.07$). The different decrease in the time constant, together with the different mean response time, suggests that the data yielded by the two algorithms provide a different picture of the phenomena occurring at the beginning of the exercise.

KEYWORDS
asymptotic standard error, fitting window, O_2 deficit, phase 1-phase 2 transition

1 | INTRODUCTION

At the start of a moderate-intensity square-wave exercise, breath-by-breath O_2 uptake ($\dot{V}_{O_2}$) as assessed at the mouth lags behind the requested mechanical power for a few minutes (Ferretti et al., 2022). Two main phases are deemed to occur throughout this transient period. The first phase (Φ_1) is believed to represent the cardiodynamic adjustment to the exercise, while the second one (Φ_2, called primary phase) is assumed to be the image of the O_2 uptake at the muscle level, and to be related to endurance performance (Bowen et al., 2019; Rossiter, 2011). Phase 2 is investigated by approximating the oxygen uptake at the mouth to a mono-exponential function and the time constant (τ) of its kinetics, obtained by the non-linear regression fitting procedure, is mostly the only evaluated parameter. However, the estimated τ might be affected by the amount of information for Φ_1 included or excluded in or from the fitting window. Theoretically, if the mono-exponential function adequately fits the time course of the original data, stable τ values should be reached after an initial decrease, as soon as the information pertaining to Φ_1 is completely excluded (Rossiter et al., 1999). However, no stable τ values were found either in clean simulated $\dot{V}_{O_2}$ data (Benson et al., 2017) or in experimental data showing a low signal-to-noise ratio (Francescato & Cettolo, 2021).

The time course of oxygen consumption at the muscle level is believed to be better approximated by the gas exchange assessed at the mouth if the changes in lung gas stores are accounted for, as occurs with the $\dot{V}_{O_2}$ values yielded by the 'Independent-breath' algorithm (Cettolo & Francescato, 2018a). This algorithm is based on the alternative view of the respiratory cycle of Grønlund (1984), and identifies the start and end points of the cycle on the basis of equal ratios between the end–tidal fractions of exchanged and not exchanged respiratory gases (Cettolo & Francescato, 2015). Conversely, the most commonly used algorithm is likely the 'Expiration-only' one (Golja et al., 2018), which calculates gas exchange from information collected only during expiration, estimating the inspiratory volume through the Haldane transformation (Roecker et al., 2005; Ward, 2018) and identifying the start and end points of the respiratory cycle from the changes in the flow direction.

Changes in lung gas stores are expected mainly at the start of a square-wave exercise (Wüst et al., 2008), and thus the use of different calculation algorithms might affect the temporal behaviour of gas exchange during this transient period. As a matter of fact, by comparing the kinetic parameters obtained for the $\dot{V}_{O_2}$ yielded by the 'Independent-breath' algorithm with those provided by more commonly available algorithms, a faster kinetics was found when all the data pertaining to the transient period were included in the fitting window (Francescato & Cettolo, 2019). In that experimentation, however, the signal-to-noise ratio was poor because only one repetition of the square-wave exercise was performed by each volunteer. It can be hypothesized that, by improving the signal-to-noise ratio, a faster kinetics will be found for the data yielded by the 'Independent-breath' algorithm compared to those of the 'Expiration-only' algorithm, even excluding from the fitting window the data pertaining to the initial time period (e.g. the data included in the first 20–25 s).

Highlights

- **What is the central question of this study?**
  Is the kinetics of breath-by-breath gas exchange at the start of a square-wave moderate intensity exercise faster when accounting for the changes in lung gas stores?
- **What is the main finding and its importance?**
  Accounting for the changes in lung gas stores, the time constant of the $\dot{V}_{O_2}$ kinetics changed less when the data pertaining to the initial period were progressively removed; time delays and mean response times were faster. Consequently, using different gas exchange calculation algorithms, the physiological phenomena occurring at the beginning of moderate-intensity exercise are characterized differently.

The aim of the present work was to test the above hypothesis by pooling together the breath-by-breath gas exchange data obtained during 10 repeated transitions performed by each volunteer, in order to increase the signal-to-noise ratio. For both algorithms, the parameters describing the timing of the kinetics were estimated several times by changing the length of the period excluded from the fitting window, in order to evaluate the effects of the inclusion/exclusion of interfering information, likely pertaining to Φ_1.

2 | METHODS

2.1 | Experimental protocol

Ten healthy and moderately active adults (5 males and 5 females) volunteered to be subjects. Their mean (± SD) age, stature and body mass were 24.6 ± 3.6 years, 1.73 ± 0.09 m, and 73.5 ± 15.1 kg, respectively. The experimental protocol, design and methods conformed to the standards set by the *Declaration of Helsinki*, except for registration in a database, and were approved by the Institutional Review Board of the Department of Medicine of the University of Udine (Italy) (no. 07/2020_IRB issued on 5 March 2020). After having been thoroughly informed about the nature, purpose and possible risks of the investigation, written informed consent was obtained by all the volunteers prior to their participation.

All the volunteers were required to have completed the Covid-19 vaccination protocol at least 15 days before the first experimental session and no one reported long-term Covid-19 symptoms. In

addition, the last experimental session of one volunteer and the first one of the next volunteer were scheduled at least 1 week apart.

Each volunteer was submitted to respiratory gas collection at the mouth while pedalling as close as possible to 60 rpm on an ergometer (Corival; Lode B.V., Groningen, the Netherlands) during: (a) 5 min pedalling at 10 W (10W-P), (b) the first bout of 6 min pedalling at ~1 W kg^{-1} body mass (moderate intensity pedalling; MI-P), (c) 10 min pedalling at 10 W, (d) the second bout of 6 min pedalling at ~1 W kg^{-1} body mass, and (e) 8 min pedalling at 10 W. Overall duration of the experimental session was thus of 35 min, during which the volunteer repeated twice the same square-wave exercise transition, each preceded by at least 5 min pedalling at 10 W. The experimental session was repeated 5 times by each volunteer, at least 1 day apart, thus allowing a total of 10 repetitions for each of them to be obtained. At the start of the first experimental session, each participant chose the cycling position that met his/her comfort requirements and the same position was subsequently used in all the following sessions.

Mechanical power, pedalling frequency, heart rate (HR), and flow ($\dot{V}$), as well as O_2 and CO_2 fractions (F_{O_2} and F_{CO_2}, respectively) in inspired and expired air at the mouth were continuously acquired throughout the trial (Metalyzer 3B, Cortex GmbH, Liepzig, Germany). The metabolic unit automatically controlled the timings of the protocol, in particular the transitions between the 10W-P and the MI-P conditions. Before each experimental session, the analysers were calibrated following the procedures indicated by the manufacturer. Mean actual mechanical power during the experimental sessions was 71.5 ± 13.1 W.

2.2 | Gas exchange calculations

Breath-by-breath oxygen consumption ($\dot{V}_{O_2}$) was calculated by means of the 'Independent-breath' algorithm (IND) according to the following equation:

$$\dot{V}_{O_2}^{IND} = -\frac{\int_{t_1}^{t_2} \dot{V} \times F_{O_2}\, dt - \frac{F_{O_2}(t_1)}{F_{N_2}(t_1)} \times \int_{t_1}^{t_2} \dot{V} \times F_{N_2}\, dt}{t_2 - t_1}. \quad (1)$$

where F_{N_2} is the instantaneous nitrogen fraction (calculated as 1 – F_{O_2} – F_{CO_2}); t_1 and t_2 correspond to the start and the end time points of the respiratory cycle, respectively, both identified on the trace of the F_{O_2}/F_{N_2} ratio (Cettolo & Francescato, 2018a).

Using the same originally acquired flow and gas fraction traces, $\dot{V}_{O_2}$ was calculated also by means of the 'Expiration-only' algorithm (EXP) according to the following equation:

$$\dot{V}_{O_2}^{EXP} = -\frac{\int_{t_e}^{t_i} \dot{V} \times F_{O_2}\, dt - \frac{F_{IO_2}}{F_{IN_2}} \times \int_{t_e}^{t_i} \dot{V} \times F_{N_2}\, dt}{t_i - t_{i-1}} \quad (2)$$

where times t_i and t_e correspond to the time points where flow changes direction and the inspiration and expiration start, respectively; and F_{IO_2} and F_{IN_2} correspond to the inspired ambient oxygen and nitrogen fractions and were set to 20.93% and 79.02%, respectively.

The software calculated automatically also breath-by-breath carbon dioxide exhalation (namely, $\dot{V}_{CO_2}^{IND}$ and $\dot{V}_{CO_2}^{EXP}$) introducing the appropriate changes into the above equations, as well as the corresponding respiratory exchange ratios (i.e., RER^{IND} and RER^{EXP}).

Both algorithms and details of the computations were described in Francescato and Cettolo (2019). As a result, three time series (namely, $\dot{V}_{O_2}$, $\dot{V}_{CO_2}$ and RER) were obtained for the IND and EXP algorithms, and thus two triplets were obtained for each experimental session for each volunteer, expressed in STPD conditions. No data were discarded (or filtered) on any of the time series before the subsequent analyses.

2.3 | Statistics on the steady states of the individual time series

All the data were analysed with the R environment (R Core Team, 2020).

For all the time series (namely, $\dot{V}_{O_2}^{IND}$, $\dot{V}_{O_2}^{EXP}$, $\dot{V}_{CO_2}^{IND}$, $\dot{V}_{CO_2}^{EXP}$, RER^{IND} and RER^{EXP}), mean values, together with the corresponding standard deviations (SD), were calculated over the following four time periods: (a) baselines BL1 and BL2, namely the last 2 min just preceding each of the two transitions between 10W-P and MI-P, and (b) steady-states SS1 and SS2, that is, the last 2 min of each of the two MI-P bouts (Figure 1).

Significant differences for the means and the SDs were assessed applying an analysis of variance for repeated measures (2 × 2 × 5 ANOVA), with the following effects: between the values obtained during BL and SS (Load effect), between the two repetitions within the same experimental session (Repetition effect), and among the five experimental sessions (Session effect), as inter-subject effects. In addition, the possible significant differences between the data yielded by the IND and the EXP algorithms were assessed (Algorithm effect). Post hoc pairwise comparison was used to detect significant differences among the various conditions.

2.4 | Data treatment and statistics on the assembled time series

For each subject and each experimental session, all the obtained $\dot{V}_{O_2}$, $\dot{V}_{CO_2}$ and RER time series were split at $t = 16$ min, and the times were shifted setting the start of the two MI-P bouts at $t = 0$. Subsequently, for each volunteer, the corresponding 10 repeated time series were assembled together using the stacking procedure (Francescato et al., 2014b).

Mean values and corresponding standard deviations were calculated over the same time periods described above, namely, for baseline (the last 2 min of 10W-P just preceding $t = 0$ s; A_b) and for steady-state (the last 2 min of MI-P just preceding $t = 360$ s; A_s). These data allowed calculation of the 'functional gain' as the ratio

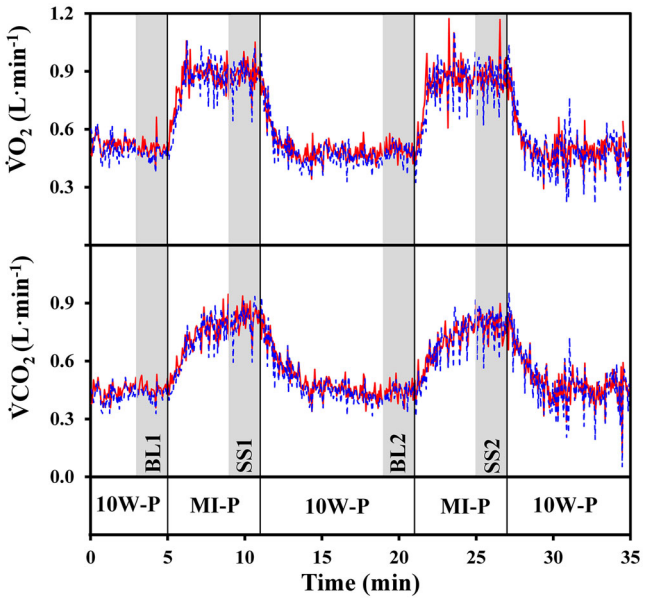

FIGURE 1 Example of gas exchange data obtained from one volunteer during an experimental session. The experimental protocol included: (a) an initial 5-min pedalling period at 10 W (10W-P), (b) two bouts of moderate intensity exercise, lasting 6 min each (1 W/kg, i.e., 55 W in this volunteer; MI-P), separated by 10 min of pedalling at 10 W, and (c) a final recovery period lasting 8 min while pedalling at 10 W. Pedalling frequency was kept as close as possible to 60 rpm throughout. $\dot{V}_{O_2}$ (upper panel) and $\dot{V}_{CO_2}$ (lower panel) data obtained applying the IND (continuous red line) or the EXP (dashed blue line) algorithms are illustrated. Vertical lines correspond to the start and end times of the two bouts of moderate-intensity pedalling periods. Shaded areas correspond to the time periods over which the data were averaged, namely, two periods during 10W-P (BL1 and BL2) and two periods during MI-P (SS1 and SS2).

between the net O_2 uptake (i.e., $A_s - A_b$) and the net mechanical power above baseline. In addition, over the same time periods, slopes of $\dot{V}_{O_2}$ against time were calculated by linear regression and their statistical significance was evaluated to assess the attainment of a steady condition.

The kinetic parameters of $\dot{V}_{O_2}$ and $\dot{V}_{CO_2}$ corresponding to the square-wave exercise transition were obtained running the non-linear regression procedure, using the R routine *nls.lm* (included in the *minpack.lm* library and minimizing the residual sum of squares by the Levenberg–Marquardt algorithm) without cleaning any outlier. The following mono-exponential model was used:

$$Y(t) = \begin{cases} A_b & t < T_d \\ A_b + \Delta A \left(1 - e^{-\frac{t-T_d}{\tau}}\right) & t \geq T_d \end{cases} \quad (3)$$

The initial values to run the iterative non-linear regression procedure were set to 25 s and 0 s for the time constant (τ) and the time delay (T_d), respectively. Baseline signal was set to A_b (as calculated above), while the initial value for the signal change (ΔA) was set to $A_s - A_b$, that is, the difference between the two signal intensities calculated above. The fitting procedure yielded the estimated values for τ, T_d and ΔA, and their asymptotic standard errors (ASE_τ, ASE_{Td} and $ASE_{\Delta A}$, respectively), which allow evaluation of the specific confidence intervals of each estimated parameter (Francescato et al., 2014a,b). In addition, the mean response time (MRT) of the overall kinetics was calculated for each data set as follows:

$$MRT = T_d + \tau. \quad (4)$$

The fitting procedure was run 51 times (always applying Equation 3), removing each time 1 s progressively longer time period (ΔT_r) from the fitting window, starting from $t = 0$ s (i.e., $\Delta T_r \in [0\text{ s}, 50\text{ s}]$). At the end of this procedure, 51 sets of estimated parameters (one for each ΔT_r) were obtained for each volunteer and for the $\dot{V}_{O_2}$ and $\dot{V}_{CO_2}$ time series obtained for the two algorithms.

Student's two-tailed *t*-test for paired data was applied for each of the different ΔT_r, to detect the statistically significant differences between the kinetic parameters obtained for the gas exchange time series provided by the two algorithms for each volunteer ($n = 10$). When a statistically significant difference was detected, its magnitude was evaluated by calculating the absolute value of the Cohen's d_Z effect size, where the Z alludes to the fact that the unit of analysis is the difference between the paired data, and the following absolute effect size classification was considered: 'trivial' < 0.2 < 'small' < 0.5 < 'medium' < 0.8 < 'large' < 1.3 < 'very large' (Lakens, 2013; Riemann & Lininger, 2018; Sullivan & Feinn, 2012).

All the statistically significant differences observed applying the parametric *t*-test were confirmed by the Wilcoxon non-parametric statistical test.

Summarized values are reported as means ± SD.

3 | RESULTS

3.1 | The experimental sessions

For all the investigated time series (calculated either by the IND and the EXP algorithms), no significant difference was observed among the mean values, or the corresponding standard deviations, when comparing the five different experimental sessions of each volunteer (repeated measures ANOVA, Session effect, $F < 1.7$, $P > 0.17$). Similarly, no significant difference was detected when comparing the two repetitions of the same experimental session (repeated measures ANOVA, Repetition effect, $F < 3.6$, $P > 0.09$). The mean values obtained for the moderate intensity pedalling condition, as well as their corresponding standard deviations, were significantly higher than those obtained for the 10W-P condition (during SS vs. BL; repeated measures ANOVA, Load effect, $F > 16.7$, $P < 0.003$), with the exception of the standard deviations for RER ($F = 1.2$, $P = 0.31$).

The mean values obtained for the IND algorithm were not significantly different from those obtained for the EXP algorithm (repeated measures ANOVA, Algorithm effect, $F < 2.2$, $P > 0.17$).

TABLE 1 Mean values and means of the corresponding standard deviations (SD) of the stacked oxygen uptake ($\dot{V}_{O_2}$), carbon dioxide exhalation ($\dot{V}_{CO_2}$) and respiratory exchange ratio (RER) data yielded by the EXP and IND algorithms, for baseline and steady state time periods.

	IND		EXP	
	Mean	SD	Mean	SD
Baseline				
$\dot{V}_{O_2}$ (l min^{-1})	0.572 (0.076)	0.082** (0.017)	0.569 (0.079)	0.099 (0.025)
$\dot{V}_{CO_2}$ (l min^{-1})	0.491 (0.062)	0.085 (0.023)	0.488 (0.063)	0.090 (0.023)
RER	0.858 (0.029)	0.081 (0.016)	0.860 (0.027)	0.055*** (0.016)
Steady state				
$\dot{V}_{O_2}$ (l min^{-1})	1.147 (0.196)	0.107*** (0.032)	1.156 (0.176)	0.148 (0.050)
$\dot{V}_{CO_2}$ (l min^{-1})	1.016 (0.159)	0.114* (0.035)	1.028 (0.142)	0.137 (0.047)
RER	0.890 (0.039)	0.074 (0.013)	0.892 (0.037)	0.043*** (0.015)
Functional gain (ml min^{-1} W^{-1})	9.3 (0.5)		9.6 (0.5)	

Note: The table summarizes also the mean values of functional gain, calculated on the basis of the individual actual mechanical power. $n = 10$ (number of volunteers). Data in brackets are the standard deviations of the corresponding mean. Statistically significant different values by comparing the IND and EXP algorithms (two-tailed paired *t*-test, $^*P < 0.05$; $^{**}P < 0.01$; $^{***}P < 0.005$). The corresponding d_Z was >0.94 for the standard deviations, and >2.86 for the RER values.

The standard deviations calculated for $\dot{V}_{O_2}^{IND}$ were significantly lower than those obtained for $\dot{V}_{O_2}^{EXP}$ (repeated measures ANOVA, Algorithm effect, $F = 20.5$, $P = 0.001$). No significant difference was detected for the $\dot{V}_{CO_2}$ values obtained with the two algorithms ($F = 4.8$, $P = 0.06$), whereas the RER^{EXP} showed significantly lower standard deviations compared to RER^{IND} ($F = 476.3$, $P < 0.001$).

Since no Repetition or Session effects were detected, the 10 time series of $\dot{V}_{O_2}$, $\dot{V}_{CO_2}$ and RER as obtained by each of the two algorithms were assembled together, thus yielding six stacked time series for each volunteer. Overall mean values and standard deviations were then calculated on the stacked time series and are summarized in Table 1, together with the corresponding 'functional gains'. No significant differences were detected between the corresponding average values ($t < 1.6$, $P > 0.14$). The standard deviations were significantly smaller for the $\dot{V}_{O_2}^{IND}$ data compared to the $\dot{V}_{O_2}^{EXP}$ data ($t > 3.5$, $P < 0.01$, $d_Z > 1.12$), independent of the exercise intensity, whereas smaller standard deviations were observed for $\dot{V}_{CO_2}^{IND}$ only during MI-P ($t = 3.0$, $P = 0.02$, $d_Z = 0.94$). Significantly smaller standard deviations were obtained for RER^{EXP} compared to RER^{IND} ($t > 9.0$, $P < 0.001$, $d_Z > 2.87$).

Attainment of a steady state condition was confirmed for all the stacked $\dot{V}_{O_2}$ time series, their slopes being never significantly different from zero ($t < 2.0$, $P > 0.05$ in all cases).

3.2 | The time period removed from the fitting window: effects on the $\dot{V}_{O_2}$ kinetic parameters

The stacked $\dot{V}_{O_2}^{IND}$ time series resulted in a faster kinetics compared to the $\dot{V}_{O_2}^{EXP}$ time series (Figure 2, left panels). As a matter of fact, up to $\Delta T_r < 16$ s significantly shorter τ values were obtained for the stacked $\dot{V}_{O_2}^{IND}$ time series ($t > 2.32$, $P < 0.046$, $d_Z > 0.73$; the difference being >4.0%). It is interesting to be noted that, between $\Delta T_r = 16$ s and $\Delta T_r = 29$ s, the time constants obtained for $\dot{V}_{O_2}^{IND}$ vs. $\dot{V}_{O_2}^{EXP}$ were not significantly different ($t < 2.05$, $P > 0.07$). Finally, for $\Delta T_r \geq 30$ s, the mean τ obtained for the stacked $\dot{V}_{O_2}^{EXP}$ time series became significantly shorter than that for $\dot{V}_{O_2}^{IND}$ ($t > 2.50$, $P < 0.034$, $d_Z > 0.79$, the difference being >9.1%). Conversely, the mean T_d (Figure 2, middle left panel) and the MRT (Figure 2, lower panel) obtained for the $\dot{V}_{O_2}^{IND}$ data were significantly shorter for all the ΔT_r values up to 50 s ($t > 2.60$, $P < 0.03$, $d_Z > 0.82$ for both parameters). The difference was greater than 17% and 8% for T_d and MRT, respectively.

The $\dot{V}_{O_2}^{IND}$ data provided more stable kinetic parameters as a function of ΔT_r. In particular, by comparing $\Delta T_r = 0$ s with $\Delta T_r = 40$ s, the mean time constants (Figure 2, upper left panel) decreased with increasing ΔT_r, with a maximum drop of 35% for the stacked $\dot{V}_{O_2}^{IND}$ time series ($t = 6.86$, $P < 0.001$, $d_Z = 2.17$) which reached 61% for the $\dot{V}_{O_2}^{EXP}$ time series ($t = 15.4$, $P < 0.001$, $d_Z = 4.86$). Focusing on the ΔT_r interval between 16 s and 29 s, the fall was still less pronounced for the $\dot{V}_{O_2}^{IND}$ data ($t = 2.82$, $P < 0.05$, $d_Z = 0.89$; drop of 10%) compared to the $\dot{V}_{O_2}^{EXP}$ data ($t = 11.18$, $P < 0.001$, $d_Z = 3.54$; drop of 23%). For both algorithms, the time delays increased by more than 100% from $\Delta T_r = 0$ s to $\Delta T_r = 40$ s ($t > 5.70$, $P < 0.001$, $d_Z > 1.80$). The resulting MRT increased significantly for the $\dot{V}_{O_2}^{EXP}$ time series ($t = 2.83$, $P = 0.02$, $d_Z = 2.66$), whereas it remained constant for the $\dot{V}_{O_2}^{IND}$ time series ($t = 1.55$, $P = 0.15$).

The mean ASE_τ values (Figure 2, upper right panel) obtained for the stacked $\dot{V}_{O_2}^{IND}$ time series were statistically lower than those for the $\dot{V}_{O_2}^{EXP}$ time series up to $\Delta T_r = 27$ s ($t > 2.53$, $P < 0.05$, $d_Z > 0.79$, the difference being >10%). The corresponding mean ASE_{Td} values (Figure 2, middle right panel) were statistically lower up to $\Delta T_r = 16$ s ($t > 2.36$, $P < 0.05$, $d_Z > 0.62$, the difference being >13%). All the mean ASE values increased with increasing ΔT_r.

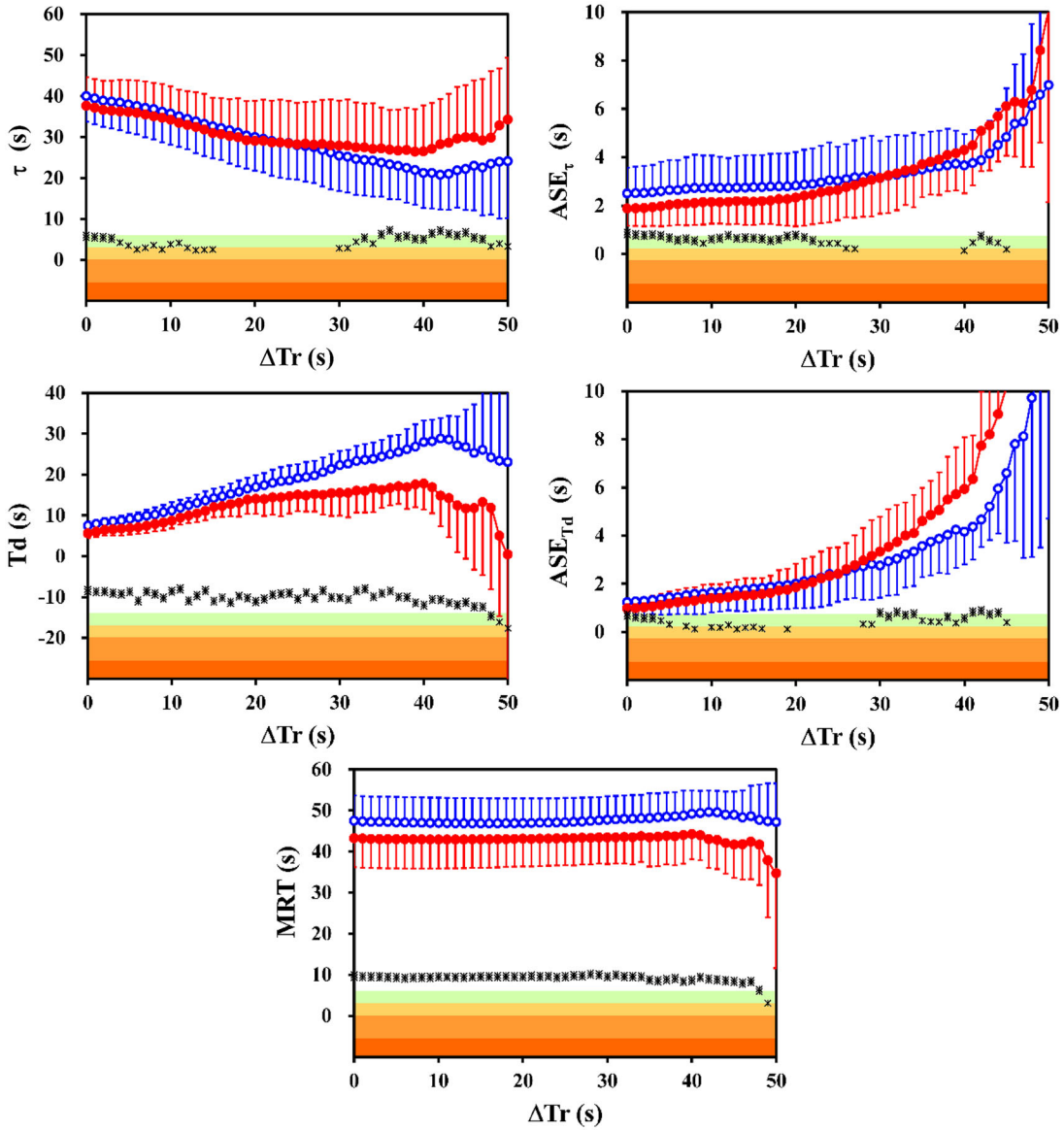

FIGURE 2 Mean time constants (τ; upper left panel) and mean time delays (T_d; middle left panel) of oxygen uptake kinetics are illustrated as a function of the time period removed from the fitting window (ΔT_r), as well as the corresponding mean asymptotic standard errors, ASE_τ (upper right panel) and ASE_{Td} (middle right panel). The corresponding mean response times (MRT) are illustrated in the lower panel. Results obtained for the data yielded by the IND (filled red circles) and the EXP (open blue circles) algorithms are illustrated in all panels. Vertical bars are the standard deviations of the individual parameters obtained running the non-linear regression procedure with the mono-exponential model. The differences between the two algorithms with the same ΔT_r are illustrated as Cohen's d_Z effect sizes (right vertical axis, on a logarithmic scale only for graphical purposes), using different symbols according to the statistical significance ($n = 10$; two-tailed paired t-test; * $P < 0.05$; ** $P < 0.01$). The 5 areas of decreasing colour intensity from bottom to top highlight the magnitude of Cohen's d_Z according to the commonly used thresholds (namely, 'trivial' < 0.2 < 'small' < 0.5 < 'medium' < 0.8 < 'large' < 1.3 < 'very large' with white background).

3.3 | The time period removed from the fitting window: effects on the $\dot{V}_{CO_2}$ kinetic parameters

The time constants of the stacked $\dot{V}^{IND}_{CO_2}$ time series were not significantly different from those of the $\dot{V}^{EXP}_{CO_2}$ time series (Figure 3, upper left panel; $t < 1.9$, $P > 0.09$). Conversely, significantly shorter time delays were detected for $\dot{V}^{IND}_{CO_2}$ up to $\Delta T_r = 40$ s ($t > 2.5$, $P < 0.04$, $d_Z > 0.70$, the difference being greater than 8.5%). Even the MRT values (Figure 3, lower panel) obtained for the $\dot{V}^{IND}_{CO_2}$ data were significantly shorter for ΔT_r up to 50 s ($t > 2.3$, $P < 0.05$, $d_Z > 0.73$), with a difference of about 3.0%.

For both algorithms, by comparing $\Delta T_r = 0$ s with $\Delta T_r = 40$ s, the mean time constants (Figure 2, upper left panel) decreased with increasing ΔT_r, with a drop of ~18% ($t > 4.34$, $P < 0.002$, $d_Z > 1.38$), the time delays increased by ~76% ($t > 3.21$, $P < 0.02$, $d_Z > 1.02$), while the resulting MRT decreased ($t > 2.75$, $P < 0.03$, $d_Z > 0.87$, drop of ~3%).

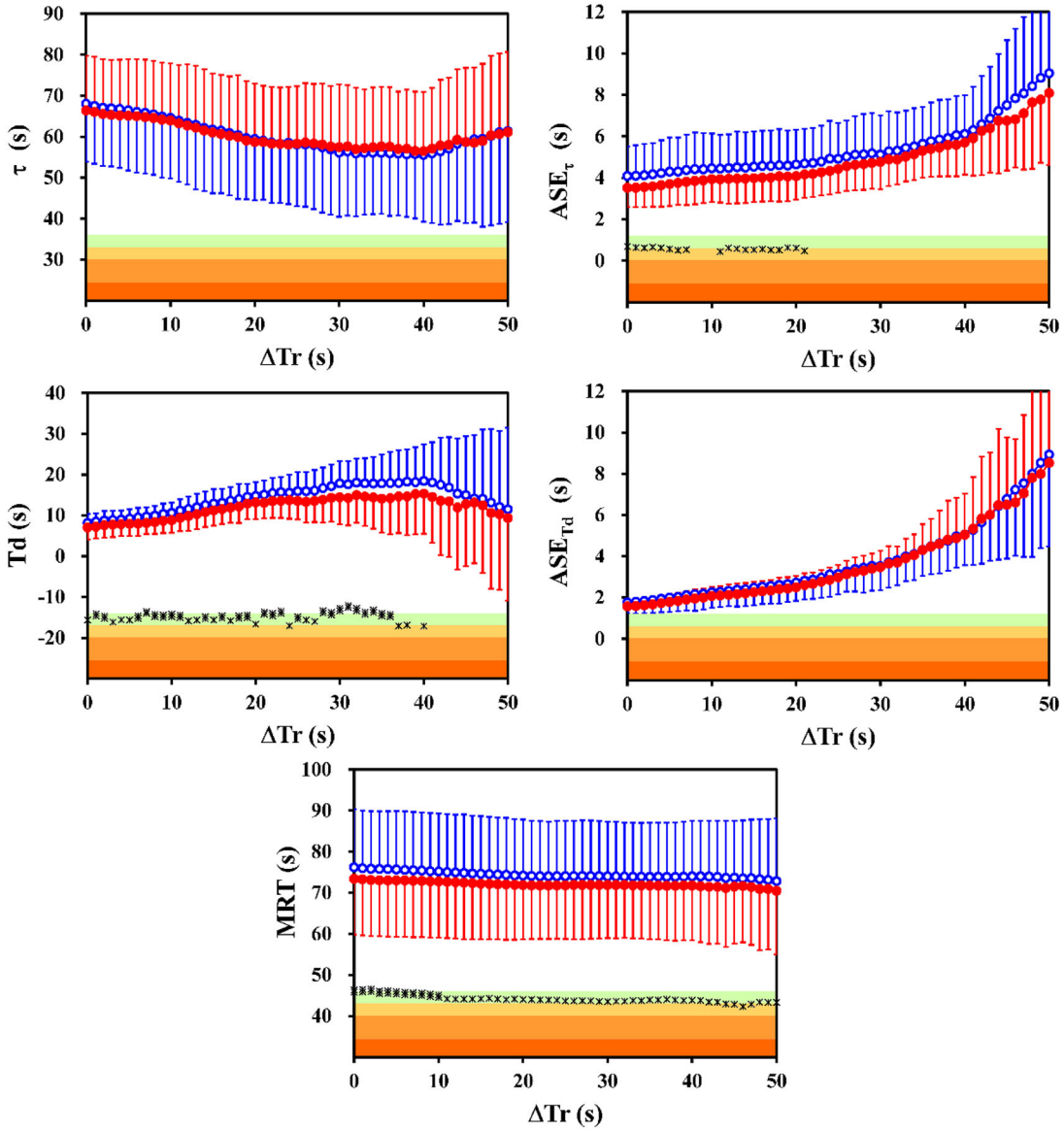

FIGURE 3 Mean time constants (τ; upper left panel) and mean time delays (T_d; middle left panel) of carbon dioxide exhalation kinetics are illustrated as a function of the time period removed from the fitting window (ΔT_r), as well as the corresponding mean asymptotic standard errors ASE_τ (upper right panel) and ASE_{Td} (middle right panel). The corresponding mean response times (MRT) are illustrated in the lower panel. Results obtained for the data yielded by the IND (filled red circles) and the EXP (open blue circles) algorithms are illustrated in all panels. Vertical bars are the standard deviations of the individual parameters obtained running the non-linear regression procedure with the mono-exponential model. The differences between the two algorithms with the same ΔT_r are illustrated as Cohen's d_Z effect sizes (right vertical axis, on a logarithmic scale only for graphical purposes), using different symbols according to the statistical significance ($n = 10$; two-tailed paired t-test; * $P < 0.05$; ** $P < 0.01$). The 5 areas of decreasing colour intensity from bottom to top highlight the magnitude of the Cohen's d_Z according to the commonly used thresholds (namely, 'trivial' < 0.2 < 'small' < 0.5 < 'medium' < 0.8 < 'large' < 1.3 < 'very large' with white background).

The mean ASE values (Figure 3, upper and middle right panels) obtained for the stacked $\dot{V}_{CO_2}^{IND}$ time series were statistically smaller than those for the $\dot{V}_{CO_2}^{EXP}$ time series only occasionally, mainly for the time constants and for ΔT_r up to 21 s. For both parameters, the mean ASE values increased with increasing ΔT_r.

4 | DISCUSSION

The main result of the present investigation was that the time parameters that characterize the oxygen uptake (or carbon dioxide exhalation) kinetics during moderate intensity exercise differed

depending on the algorithm used to calculate the gas exchange data. In particular, our results suggest that the temporal behaviour of the $\dot{V}_{O_2}^{IND}$ data, compared to that of $\dot{V}_{O_2}^{EXP}$ data, resulted in a steadier time constant upon removing increasing time periods from the fitting window. Moreover, the $\dot{V}_{O_2}^{IND}$ data showed a faster overall kinetics, as suggested by a shorter mean response time.

4.1 | Comparison of the two algorithms under steady conditions

In the present experimentation the IND and EXP algorithms provided similar mean gas exchange values despite the EXP algorithm (Equation 2) was neglecting the dead space of the breathing apparatus. It should be noted, however, that the latter adjustment as proposed by Beaver et al. (1973) is under debate, considering that it should account even for breathing frequency and/or tidal volume (Ward, 2018). The mean oxygen uptake values are in agreement with the literature. Indeed, applying Equation 4 of Formenti et al. (2015), the estimated $\dot{V}_{O_2}$ will amount to 1.15 litres min^{-1}, which is practically equal to the values reported in Table 1 (~1.16 litres min^{-1}). Moreover, the 'functional gain' of the responses (~9.5 ml min^{-1} W^{-1}) is not far from 9.47 ± 0.85 and ~10.0 ml min^{-1} W^{-1}, as reported by Benson et al. (2017) and Rossiter (2011), respectively. Although we are aware that the RER values are affected by the duration of fasting before the exercise (Liu & Chen, 2022), no attention was paid to performing all the experimental sessions at the same day time, since RER was not a main outcome. The obtained RER values, however, were in line with the values reported in the literature for similar exercise conditions (Baldassarre et al., 2022; Liu & Chen, 2022; Miyamoto et al., 2022).

As already observed under several different exercise conditions (Cettolo & Francescato, 2018a; Francescato & Cettolo, 2019; Koschate et al., 2019), the standard deviations of the $\dot{V}_{O_2}^{IND}$ values during steady conditions were significantly lower than those of $\dot{V}_{O_2}^{EXP}$. Indeed, the IND algorithm accounts for the changes of the pulmonary O_2 stores, which typically occur for the anomalous breaths (Francescato et al., 2019), thus reducing the fluctuations around the mean of the oxygen consumption as measured at the mouth.

Similar standard deviations were observed between the $\dot{V}_{CO_2}^{IND}$ and $\dot{V}_{CO_2}^{EXP}$ values, in particular at rest. It is to be noted, however, that the alveolar CO_2 stores are dynamically balanced with the amount of HCO_3^- dissolved in the blood (Cettolo & Francescato, 2018b); accordingly, when an anomalous breath occurs, the CO_2 lung stores might remain quite constant, making negligible the correction for their changes.

4.2 | The $\dot{V}_{O_2}$ ON transient phase

Theoretically, as soon as all the information pertaining to Φ_1 is excluded, the behaviour of the time constant of $\dot{V}_{O_2}$ as a function of ΔT_r should reach a stable value (Rossiter et al., 1999). This behaviour was not followed by the mean τ value of $\dot{V}_{O_2}^{EXP}$ of the present investigation, which continued decreasing up to $\Delta T_r \approx 40$ s. Conversely, a rather stable mean τ value for $\dot{V}_{O_2}^{IND}$ was observed for $\Delta T_r > 16$ s suggesting that, for these fitting windows, information pertaining to phase 1 was likely excluded. Since the flow and gas traces, as collected at the mouth, were the same for the calculations with both algorithms, it could be expected that the cardiodynamic adjustment to the exercise (e.g. the increase in cardiac output) would be excluded for the same ΔT_r, which was not the case. Consequently, the observed discrepancy can be explained only by the fact that the two algorithms account (or not) for the changes in lung gas stores in their calculations.

The model commonly used to estimate the kinetic parameters by non-linear regression includes also the time delay, which mathematically is the back projection of the fitted data to the baseline. This parameter is correlated to the Φ_1 to Φ_2 transition time, although it does not correspond to the latter (Rossiter, 2011). However, it should be noted that the sum of T_d and τ reflects the MRT of the overall O_2 uptake kinetics during the transient and allows calculation of the O_2 deficit (O_{2def}) as follows (Whipp et al., 1982):

$$O_{2def} = \Delta A \times (T_d + \tau) = \Delta A \times MRT. \quad (5)$$

Accordingly, there is a direct proportion between MRT and O_2 deficit with equal ΔA (i.e. the net increase in O_2 uptake at the asymptote). The O_{2def} includes the changes in the pulmonary O_2 stores, which are theoretically compensated for by the IND algorithm. A faster MRT can thus be expected for the data of the IND algorithm compared to the EXP one, as was observed in the present work (43.3 ± 7.1 s vs. 47.5 ± 6.2 s).

The O_2 deficit is a physiological variable that should be independent of the amount of information used by the non-linear fitting procedure. Consequently, a quite constant MRT should be predicted irrespective of ΔT_r, as was the case for both algorithms up to $\Delta T_r \approx 40$ s (Figure 2, lower panel), mainly because of complementary time constants and time delays.

For all the estimated parameters, the asymptotic standard error, namely the statistical descriptor that allows evaluation of the confidence intervals of the corresponding estimated value (Francescato et al., 2014a,b), increased on average with increasing ΔT_r, likely because fewer data points were included in the non-linear regression. Smaller ASE values were obtained for $\dot{V}_{O_2}^{IND}$ compared to $\dot{V}_{O_2}^{EXP}$, in particular for the smaller ΔT_r (Figure 2, right panels). These results suggest that the IND algorithm provides less noisy gas exchange data also during the transient phases and/or the $\dot{V}_{O_2}^{IND}$ data fit better the mono-exponential model.

4.3 | The $\dot{V}_{CO_2}$ ON transient phase

To the best of our knowledge, the kinetics of carbon dioxide exhalation at the start of a moderate intensity exercise has received much less attention in the literature compared to the kinetics of oxygen

uptake, despite its providing insights into the inherent control features of ventilation and gas exchange (Ward et al., 2023; Whipp et al., 1982). It can be hypothesized that the cardiodynamic adjustment at the beginning of the exercise affects also the breath-by-breath $\dot{V}_{CO_2}$ values, involving changes in lung gas stores. Indeed, similar to the behaviour of the kinetic parameters of $\dot{V}_{O_2}$, in the present investigation, the time constant of $\dot{V}_{CO_2}$ decreased with increasing ΔT_r, while the T_d increased (Figure 3, left panels). Nevertheless, no quite steady $\dot{V}_{CO_2}$ kinetic parameters were found by removing from the fitting window 1-s longer initial periods, suggesting that the behaviour of $\dot{V}_{CO_2}$ at the start of the exercise departs from the mono-exponential function much more than the kinetics of $\dot{V}_{O_2}$.

In addition, results of the present work suggest that the changes in lung CO_2 stores are less pronounced compared to the changes in lung O_2 stores (both accounted for by the IND algorithm). Indeed, these changes were not sufficient to affect the values of the $\dot{V}_{CO_2}$ time constant, and/or the corresponding ASE values, which were not significantly different between the two algorithms at stake for the majority of the explored ΔT_r. The lung CO_2 stores, however, changed to an extent detectable by the IND algorithm, and influenced slightly the start of the kinetics, resulting in a lower time delay and/or mean response time.

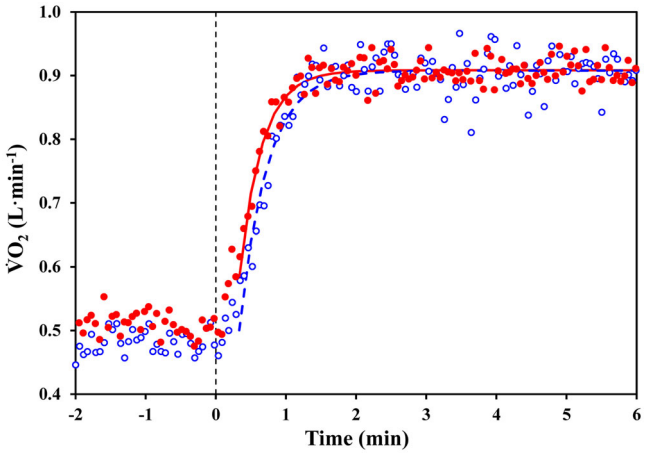

FIGURE 4 Stacked $\dot{V}_{O_2}^{IND}$ (filled red circles; continuous line) and $\dot{V}_{O_2}^{EXP}$ (open blue circles; dashed line) time series of the same subjects as in Figure 1. For graphical purposes, data of the 10 repetitions pertaining to the same algorithm were first stacked together, sorted in ascending time and then averaged both in time and in signal intensity over 10 consecutive data points (i.e. the number of repetitions). For both algorithms, the parameters estimated by non-linear regression with $\Delta T_r = 20$ s were used to draw the two lines showing the corresponding kinetics.

4.4 | The commonly used procedure of analysis

Focusing specifically on the arbitrary time period excluded by the vast majority of those estimating $\dot{V}_{O_2}$ kinetics (i.e., $\Delta T_r = 20$ s, which does not necessarily correspond to the Φ_1 to Φ_2 transition time), no significant difference in the average time constant was detected between the $\dot{V}_{O_2}^{IND}$ and $\dot{V}_{O_2}^{EXP}$ data (29.0 ± 9.8 s vs. 30.0 ± 8.2 s, respectively). These averages might lead to the conclusion that there is no effective difference between using the IND or EXP algorithms. It cannot be excluded, however, that the similarity of the τ estimated for the data provided by the two algorithms with $\Delta T_r \approx 20$ s was observed by chance, or it is linked to the characteristics (among which age and training level) of the recruited subjects. Indeed, phase 1 in older volunteers can be as long as 35 s (Mezzani et al., 2010), and thus the data of the two algorithms might produce significantly different time constants at ΔT_r of 20 s. Despite the similar time constants, it is not possible to neglect the significantly shorter T_d for the IND algorithm (14.1 ± 3.6 s vs. 16.9 ± 2.9 s, for $\dot{V}_{O_2}^{IND}$ and $\dot{V}_{O_2}^{EXP}$, respectively), which is suggestive of a faster overall kinetics. Figure 4 illustrates the two stacked $\dot{V}_{O_2}$ time series of the same subject as for Figure 1, together with the regression lines corresponding to the two kinetics obtained for $\Delta T_r = 20$ s. It clearly appears that the kinetics for the $\dot{V}_{O_2}^{IND}$ data were faster compared to the $\dot{V}_{O_2}^{EXP}$ data. Only for graphical reasons, in Figure 4 the data of the 10 repetitions were first stacked together, sorted in ascending time and then averaged both in time and in signal intensity over 10 consecutive data points (i.e. the number of repetitions). Finally, it should be noted that, for $\Delta T_r = 20$ s, the $\dot{V}_{O_2}^{IND}$ data resulted in smaller ASE values, suggesting that the corresponding estimated parameters are more precise (Figure 2 right panels).

In the present experimentation, volunteers repeated 10 times the same exercise transient. Nevertheless, when the number of repetitions was limited to four, as suggested by Benson et al. (2017), results were comparable to those obtained on 10 repeated bouts, as concerned all the investigated areas, that is, the mean values and corresponding standard deviations, the statistically significant differences between the two algorithms, and, finally, the behaviours according to the excluded time period (ΔT_r). As expected, however, the average ASE values obtained for the data yielded by both algorithms were somewhat greater than those obtained for 10 repetitions, while the $\dot{V}_{O_2}^{IND}$ data still resulted in lower ASE values compared to the $\dot{V}_{O_2}^{EXP}$ data (data not shown).

4.5 | Fraction of pulmonary O_2 stores accounted for by the IND algorithm

As already stated above, the MRT of $\dot{V}_{O_2}$ at the start of a square-wave exercise of moderate intensity allows calculation of the O_2 deficit (Whipp et al., 1982). A smaller O_2 deficit could be estimated for the $\dot{V}_{O_2}^{IND}$ data compared to the $\dot{V}_{O_2}^{EXP}$ data (i.e., ~420 mL vs. ~470 mL), because of the ~10% difference between the MRT values obtained for the two algorithms. The difference of ~50 mL in the O_2 deficit might be associated to the changes in lung O_2 stores, likely accounted for by the IND algorithm, but not by the EXP one. This volume might seem small and thus negligible, but this is not the case, since it represents about 56% of the overall changes in the pulmonary O_2 stores (50 mL/90 mL).

Indeed, the overall changes in pulmonary O_2 stores (~90 mL) were estimated assuming that: (a) the splitting of the high-energy

phosphates is the mirror image of oxygen consumption at the muscle level (Ferretti et al., 2022; Rossiter et al., 1999), with a time constant of 25 s without any time delay (Barker et al., 2008; Francescato et al., 2013; Jones et al., 2008), and (b) the changes in the venous blood O_2 stores can be estimated according to the arterio- to mixed venous blood oxygen difference at rest and at steady state (Francescato et al., 2003), using the values reported for an exercise similar to that of the present investigation (Fontolliet et al., 2021).

4.6 | Strengths and limitations

Volunteers started abruptly the moderate intensity exercise bout after a 10-W pedalling period, ensuring that the increase in O_2 uptake was essentially due to the increase in mechanical power and not to the inertial effects of the ergometer flywheel at exercise onset (Whipp et al., 1982) or to the work needed to move the limbs (Francescato et al., 1995). Even possible interferences of anticipation were avoided (Miyamoto et al., 2022), since volunteers were not informed about the timings of the protocol, in particular of the changes in workload, that were automatically set by the software of the metabolic unit. This allowed us to circumvent the need to apply manual re-alignments specific for each volunteer.

Exercise intensity was chosen according to volunteer's body mass, not relative to an individual physiological threshold during exercise (e.g. gas exchange threshold or lactate threshold). During a constant intensity exercise below the above thresholds, however, following the cardiodynamic phase and the primary phase, gas exchange remains quite constant and does not show a temporal drift (the so-called slow component). The non-statistically significant slopes found in the gas exchange data during steady-state are suggestive of the absence of a slow component in all the volunteers. Moreover, since the same original flow and gas fraction traces were used to calculate gas exchange by means of the two algorithms, the slow component would have had a similar effect on whatever kinetic parameter (e.g. lengthening the time constant) obtained for both algorithms.

Each volunteer repeated 10 times the same moderate intensity pedalling bout and repeatable data were collected making us confident that our experimental data show an adequate signal-to-noise ratio for kinetic analyses. Moreover, the different repetitions were stacked, without discarding or filtering the originally acquired data, maintaining the validity and meaning of every single value in determining the kinetic parameters and the corresponding uncertainty (Francescato et al., 2014b, 2015, 2017).

The group of volunteers was rather uniform in age, allowing us to obtain more homogeneous results and to make inferences on the basis of literature data for volunteers of similar characteristics (i.e., the phosphocreatine breakdown time constant and the arterio- to mixed venous blood oxygen difference at rest and during exercise). Conversely, the narrow range of ages might be considered a limitation, since older subjects might lead to different results.

Finally, the comparison of gas exchange kinetic parameters for $\dot{V}_{O_2}$ data obtained with different calculation methods/algorithms has led to contrasting results (e.g., Aliverti et al., 2009; Beaver et al., 1981; Cautero et al., 2002), likely because of different experimental protocols (e.g. different baselines) and/or methods of analysis (e.g. fitting with a bi-exponential model). Consequently, a systematic comparison with our results could only introduce further confusion.

It remains to be evaluated whether the two algorithms at stake might show a different sensitivity in detecting intervention-induced changes in the gas exchange kinetic parameters (e.g. exercise training). It can be expected that the IND algorithm might detect differently the interventions that change the $\Phi_1\Phi_2$ transition time and/or that change the involvement of the lung gas stores.

4.7 | Conclusions

Results of the present investigation suggest that, using a mono-exponential model, the kinetic parameters of breath-by-breath oxygen uptake and carbon dioxide exhalation might differ depending on whether gas exchange is calculated accounting for the changes in lung gas stores or not. The IND and EXP algorithms resulted in comparable oxygen uptake time constants only for a portion of the investigated fitting windows (i.e., for ΔT_r between 16 s and 29 s), while the time constants of carbon dioxide exhalation were comparable at all the investigated ΔT_r. Nevertheless, the IND algorithm yielded significantly faster mean response times for $\dot{V}_{O_2}$ over the whole range of investigated ΔT_r, to which corresponded a smaller O_2 deficit. Consequently, the physiological phenomena occurring at the start of a moderate intensity exercise might be interpreted differently according to the gas exchange calculation algorithm used.

AUTHOR CONTRIBUTIONS

Maria Pia Francescato and Valentina Cettolo contributed in conception and design of the experiments; both performed the experiments, analysed the data and wrote the paper. All authors have read and approved the final version of this manuscript and agree to be accountable for all aspects of the work in ensuring that questions related to the accuracy or integrity of any part of the work are appropriately investigated and resolved. All persons designated as authors qualify for authorship, and all those who qualify for authorship are listed.

ACKNOWLEDGEMENTS

We thank Cortex GmbH (Leipzig, Germany) for having provided us with the metabolic unit. Cortex GmbH was not involved in the study design, data collection, analysis or interpretation.

CONFLICT OF INTEREST

The authors declare no conflicts of interest.

DATA AVAILABILITY STATEMENT

Data supporting the findings of the present paper as well as the software used are available from the corresponding author upon reasonable request.

ORCID

Maria Pia Francescato https://orcid.org/0000-0002-7892-863X
Valentina Cettolo https://orcid.org/0000-0003-0577-1317

REFERENCES

Aliverti, A., Kayser, B., Cautero, M., Dellaca, R. L., di Prampero, P. E., & Capelli, C. (2009). Pulmonary VO_2 kinetics at the onset of exercise is faster when actual changes in alveolar O_2 stores are considered. *Respiratory Physiology & Neurobiology*, *169*, 78–82.

Baldassarre, G., Zuccarelli, L., Manferdelli, G., Manfredini, V., Marzorati, M., Pilotto, A., Porcelli, S., Rasica, L., Šimunič, B., Pišot, R., Narici, M., & Grassi, B. (2022). Decrease in work rate in order to keep a constant heart rate: Biomarker of exercise intolerance following a 10-day bed rest. *Journal of Applied Physiology*, *132*, 1569–1579.

Barker, A. R., Welsman, J. R., Fulford, J., Welford, D., & Armstrong, N. (2008). Muscle phosphocreatine kinetics in children and adults at the onset and offset of moderate-intensity exercise. *Journal of Applied Physiology*, *105*, 446–456.

Beaver, W. L., Lamarra, N., & Wasserman, K. (1981). Breath-by-breath measurement of true alveolar gas exchange. *Journal of Applied Physiology: Respiratory, Environmental and Exercise Physiology*, *51*, 1662–1675.

Beaver, W. L., Wasserman, K., & Whipp, B. J. (1973). On-line computer analysis and breath-by-breath graphical display of exercise function tests. *Journal of Applied Physiology*, *34*, 128–132.

Benson, A., Bowen, T., Ferguson, C., Murgatroyd, S., & Rossiter, H. B. (2017). Data collection, handling and fitting strategies to optimize accuracy and precision of oxygen uptake kinetics estimation from breath-by-breath measurements. *Journal of Applied Physiology*, *123*, 227–242.

Bowen, T. S., Benson, A. P., & Rossiter, H. B. (2019). Chapter 10 - The coupling of internal and external gas exchange during exercise. In J. A. Zoladz (Ed.), *Muscle and Exercise Physiology*. Academic Press (pp. 217–249).

Cautero, M., Beltrami, A. P., di Prampero, P. E., & Capelli, C. (2002). Breath-by-breath alveolar oxygen transfer at the onset of step exercise in humans: Methodological implications. *European Journal of Applied Physiology*, *88*, 203–213.

Cettolo, V., & Francescato, M. P. (2015). Assessment of breath-by-breath alveolar gas exchange: An alternative view of the respiratory cycle. *European Journal of Applied Physiology*, *115*, 1897–1904.

Cettolo, V., & Francescato, M. P. (2018a). Assessing breath-by-breath alveolar gas exchange: Is the contiguity in time of breaths mandatory? *European Journal of Applied Physiology*, *118*, 1119–1130.

Cettolo, V., & Francescato, M. P. (2018b). Effects of abrupt changes in lung gas stores on the assessment of breath-by-breath gas exchange. *Clinical Physiology and Functional Imaging*, *38*, 491–496.

Ferretti, G., Fagoni, N., Taboni, A., Vinetti, G., & di Prampero, P. E. (2022). A century of exercise physiology: Key concepts on coupling respiratory oxygen flow to muscle energy demand during exercise. *European Journal of Applied Physiology*, *122*, 1317–1365.

Fontolliet, T., Bringard, A., Adami, A., Fagoni, N., Tam, E., Taboni, A., & Ferretti, G. (2021). Vagal blockade suppresses the phase I heart rate response but not the phase I cardiac output response at exercise onset in humans. *European Journal of Applied Physiology*, *121*, 3173–3187.

Formenti, F., Minetti, A. E., & Borrani, F. (2015). Pedaling rate is an important determinant of human oxygen uptake during exercise on the cycle ergometer. *Physiological Reports*, *3*, e12500.

Francescato, M., Cettolo, V., & Bellio, R. (2014a). Confidence intervals for the parameters estimated from simulated O_2 uptake kinetics: Effects of different data treatments. *Experimental Physiology*, *99*, 187–195.

Francescato, M. P., & Cettolo, V. (2019). The "independent breath" algorithm: Assessment of oxygen uptake during exercise. *European Journal of Applied Physiology*, *119*, 495–508.

Francescato, M. P., & Cettolo, V. (2021). Influence of the fitting window on the O_2 uptake kinetics at the onset of moderate intensity exercise. *Journal of Applied Physiology*, *131*, 1009–1019.

Francescato, M. P., Cettolo, V., & Bellio, R. (2014b). Assembling more O_2 uptake responses: Is it possible to merely stack the repeated transitions? *Respiratory Physiology & Neurobiology*, *200*, 46–49.

Francescato, M. P., Cettolo, V., & Bellio, R. (2015). Interpreting the confidence intervals of model parameters of breath-by-breath pulmonary O_2 uptake. *Experimental Physiology*, *100*, 475.

Francescato, M. P., Cettolo, V., & Bellio, R. (2017). Interpreting the averaging methods to estimate oxygen uptake kinetics parameters. *Journal of Applied Physiology*, *123*, 1018–1018.

Francescato, M. P., Cettolo, V., & Di Prampero, P. E. (2003). Relationships between mechanical power, O(2) consumption, O(2) deficit and high-energy phosphates during calf exercise in humans. *Pflugers Archiv: European Journal of Physiology*, *445*, 622–628.

Francescato, M. P., Cettolo, V., & di Prampero, P. E. (2013). Oxygen uptake kinetics at work onset: Role of cardiac output and of phosphocreatine breakdown. *Respiratory Physiology & Neurobiology*, *185*, 287–295.

Francescato, M. P., Girardis, M., & di Prampero, P. E. (1995). Oxygen cost of internal work during cycling. *European Journal of Applied Physiology and Occupational Physiology*, *72*, 51–57.

Francescato, M. P., Thieschäfer, L., Cettolo, V., & Hoffmann, U. (2019). Comparison of different breath-by-breath gas exchange algorithms using a gas exchange simulation system. *Respiratory Physiology & Neurobiology*, *266*, 171–178.

Golja, P., Cettolo, V., & Francescato, M. P. (2018). Calculation algorithms for breath-by-breath alveolar gas exchange: The unknowns!. *European Journal of Applied Physiology*, *118*, 1869–1876.

Grønlund, J. (1984). A new method for breath-to-breath determination of oxygen flux across the alveolar membrane. *European Journal of Applied Physiology*, *52*, 167–172.

Jones, A. M., Wilkerson, D. P., & Fulford, J. (2008). Muscle [phosphocreatine] dynamics following the onset of exercise in humans: The influence of baseline work-rate. *The Journal of Physiology*, *586*, 889–898.

Koschate, J., Cettolo, V., Hoffmann, U., & Francescato, M. P. (2019). Breath-by-breath oxygen uptake during running: Effects of different calculation algorithms. *Experimental Physiology*, *104*, 1829–1840.

Lakens, D. (2013). Calculating and reporting effect sizes to facilitate cumulative science: A practical primer for t-tests and ANOVAs. *Frontiers in Psychology*, *4*, 863.

Liu, M.-Y., & Chen, S.-Q. (2022). Effects of low/medium-intensity exercise on fat metabolism after a 6-h fast. *International Journal of Environmental Research and Public Health*, *19*, 15502.

Mezzani, A., Grassi, B., Giordano, A., Corrà, U., Colombo, S., & Giannuzzi, P. (2010). Age-related prolongation of phase I of VO_2 on-kinetics in healthy humans. *American Journal of Physiology. Regulatory, Integrative and Comparative Physiology*, *299*, R968–R976.

Miyamoto, T., Sotobayashi, D., Ito, G., Kawai, E., Nakahara, H., Ueda, S., Toyama, T., Saku, K., Nakanishi, Y., & Kinoshita, H. (2022). Physiological role of anticipatory cardiorespiratory responses to exercise. *Physiological Reports*, *10*, e15210.

R Core Team. (2020). *R: A Language and Environment for Statistical Computing*. R Foundation for Statistical Computing.

Riemann, B. L., & Lininger, M. R. (2018). Principles of statistics: What the sports medicine professional needs to know. *Clinics in Sports Medicine*, *37*, 375–386.

Roecker, K., Prettin, S., & Sorichter, S. (2005). Gas exchange measurements with high temporal resolution: The breath-by-breath approach. *International Journal of Sports Medicine*, *26*(1), S11–S18.

Rossiter, H. B. (2011). Exercise: Kinetic considerations for gas exchange. *Comprehensive Physiology*, *1*, 203–244.

Rossiter, H. B., Ward, S. A., Doyle, V. L., Howe, F. A., Griffiths, J. R., & Whipp, B. J. (1999). Inferences from pulmonary O_2 uptake with respect to intramuscular [phosphocreatine] kinetics during moderate exercise in humans. *The Journal of Physiology*, *518*, 921–932.

Sullivan, G. M., & Feinn, R. (2012). Using effect size-or why the p value is not enough. *Journal of Graduate Medical Education*, *4*, 279–282.

Ward, A. M. M., Guluzade, N. A., Kowalchuk, J. M., & Keir, D. A. (2023). Coupling of V ˙E and V ˙CO_2 kinetics: Insights from multiple exercise transitions below the estimated lactate threshold. *European Journal of Applied Physiology*, *123*, 509–522.

Ward, S. A. (2018). Open-circuit respirometry: Real-time, laboratory-based systems. *European Journal of Applied Physiology*, *118*, 875–898.

Whipp, B. J., Ward, S. A., Lamarra, N., Davis, J. A., & Wasserman, K. (1982). Parameters of ventilatory and gas exchange dynamics during exercise. *Journal of Applied Physiology: Respiratory, Environmental and Exercise Physiology*, *52*, 1506–1513.

Wüst, R. C. I., Aliverti, A., Capelli, C., & Kayser, B. (2008). Breath-by-breath changes of lung oxygen stores at rest and during exercise in humans. *Respiratory Physiology & Neurobiology*, *164*, 291–299.

How to cite this article: Francescato, M. P., & Cettolo, V. (2024). The algorithm used for the calculation of gas exchange affects the estimation of O_2 uptake kinetics at the onset of moderate-intensity exercise. *Experimental Physiology*, *109*, 393–404. https://doi.org/10.1113/EP091146